

## Direct Position Analysis of a Large Family of Spherical and Planar Parallel Manipulators with Four Loops

JÚLIA BORRÀS

*Institut de Robòtica i Informàtica Industrial (UPC-CSIC)  
Barcelona, Spain  
jborras@iri.upc.edu*

RAFFAELE DI GREGORIO(\*)

*Department of Engineering (EnDiF) - University of Ferrara  
Ferrara, Italy  
rdigregorio@ing.unife.it*

(\*) Corresponding author

**Abstract:** *The direct position analysis (DPA) of a manipulator is the computation of the end-effector poses (positions and orientations) compatible with assigned values of the actuated-joint variables. Assigning the actuated-joint variables corresponds to considering the actuated joints locked, which makes the manipulator a structure. The solutions of the DPA of a manipulator one-to-one correspond to the assembly modes of the structure that is generated by locking the actuated-joint variables of that manipulator. Determining the assembly modes of a structure means solving the DPA of a large family of manipulators since the same structure can be generated from different manipulators. This paper provides an algorithm that determines all the assembly modes of two structures with the same topology which are generated from two families of mechanisms: one planar and the other spherical. The topology of these structures is constituted of nine links (one quaternary link, four ternary links and four binary links) connected through twelve revolute pairs to form four closed loops.*

### 1 Introduction

The direct position analysis (DPA) of a manipulator is the computation of the end-effector poses (positions and orientations) compatible with assigned values of the actuated-joint variables. Assigning the actuated-joint variables corresponds to considering the actuated joints locked, which makes the manipulator a structure. The solutions of the DPA of a manipulator one-to-one correspond to the assembly modes of the structure generated by locking the actuated-joint variables of that manipulator. Determining the assembly modes of a structure means solving the DPA of a large family of manipulators since the same structure can be generated from different manipulators.

The solution of the DPA of parallel manipulators (PMs) is a difficult and challenging task since, in general, it involves the solution of a system of non-linear equations.

Spherical parallel manipulators (SPMs) are PMs where the end-effector performs only spherical motions with a center fixed to the frame. SPMs can be collected into two subsets: (i) the set of the SPMs where only the end-effector and few (or no) other links perform spherical motions with the same center, and (ii) the set of the SPMs where all the links perform spherical motions with the same center. When the actuated joints are locked, both these two types of SPMs become structures whose assembly modes can be identified by considering equivalent structures where the links are connected only through revolute pairs with axes that converge toward the spherical motion center. Such structures will be called spherical structures (SSs).

Structures composed of links connected only through revolute pairs are also generated from a large family of planar parallel manipulators (PPMs) by locking the actuated joints. In this case, all the revolute pair axes are parallel to one another, and perpendicular to the plane of motion. Such structures will be called planar structures (PSs).

When the topology of a structure is analyzed, only the number and the type (binary, ternary, etc.) of links, and the type of kinematic pairs that connect the links to one another are considered. Therefore, the SSs and the PSs share the same set of topologies.

Moreover, by using the Grübler-Kutzbach equation, it is easy to demonstrate that, in the SSs and the PSs, the number of loops,  $l$ , the number of links,  $m$ , and the number of revolute pairs,  $r$ , are related by the following two relationships:  $m = 2l + 1$ ;  $r = 3l$ .

Sometimes structures contain substructures (i.e. an subset of links that form a structure by themselves). A substructure can be substituted into the original structure by a unique link whose shape depend on the assembly modes of the substructure. This substitution process ends when no other substructure can be identified in the last obtained structure. In the literature, structures that do not contain substructure have been called Assur kinematic chains (AKCs). The determination of all the assembly modes of

any structure can be implemented by exploiting a set of algorithms that solve all the AKCs (Innocenti (1995)).

The solution of the DPA of all the SPMs can be implemented by classifying all the SS topologies which refer to AKCs, and, then, by providing, for each identified topology, an algorithm that computes the assembly modes of the AKC with that topology. The fact that the set of SS topologies coincides with the one of PSs allows the wide literature on planar mechanisms to be exploited (Wampler (2004)). In particular (see Innocenti (1995)), there are one single-loop AKC topology (the triad), one double-loop AKC topology (the pentad), and three triple-loop AKC topologies. Moreover, Manolescu (1973) gave a complete classification of triple-loop topologies and how they are built. Eventually, Shen *et al.* (2000) identified all the AKC topologies with up to four loops. So doing, they showed that there are 28 quadruple-loop AKC topology.

The algorithms that analytically calculate all the assembly modes of the AKCs up to three loops have been already presented both for the planar case (see Innocenti (1995) for the Refs.), and for the spherical case (see Wampler (2004) for the Refs.).

This paper addresses the determination of the assembly modes of the structures, either planar or spherical, with one out of the 28 quadruple-loop AKC topologies. And it provides one algorithm, which is applicable to the planar and the spherical cases and solves the closure-equation systems of these structures in analytical form. In particular, the topology of these structures is the one reported in Fig. 1, and it is constituted of nine links (one quaternary link, four ternary links and four binary links) connected through twelve revolute pairs to form four closed loops.

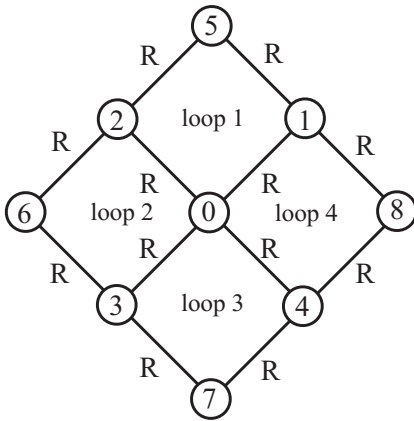


Figure 1: Topology of the studied structures: graph vertices represent links, graph edges represent joints (R stands for revolute pair).

## 2 Basic concepts

The closure equations of a structure (or a mechanism) can be written in many ways. The most common techniques are based on the use of the loop equations which are a fixed number, say  $n$ , of independent scalar equations that can be written for each independent loop appearing in the structure.

When the structure contains a number of particular binary

links at least equal to the number of independent loops, and the choice of the independent loops can be operated so that each loop contains at least one binary link not included in the other loops, the number  $n$  can be reduced to one, and the closure-equation system can be reduced to a number of scalar equations equal to the number of loops.

The analysis of Fig. 1 reveals that, in the structures under study, four independent loops with one binary link can be easily individuated: (1) loop 0-1-5-2 (link 5 is binary), (2) loop 0-2-6-3 (link 6 is binary), (3) loop 0-3-7-4 (link 7 is binary), and (4) loop 0-4-8-1 (link 8 is binary). All these loops are four-bar loops with only revolute pairs.

Both in the planar case and in the spherical case, the revolute pair axes are located by points lying on the motion plane<sup>1</sup> (planar case) or on the unit sphere<sup>2</sup> (spherical case). In our case, this technique simply consist in writing, for each loop, that the distance (either on the motion plane or on the unit sphere<sup>3</sup>) between the two points locating the revolute-pair axes at the endings of the binary link is constant.

In the next sections this technique will be used to write a minimal set of closure equations both for the planar case and for the spherical case.

## 3 Closure equations

By using the above-mentioned technique to write the closure equations, the resulting closure equations are very similar in the two cases under study, and the same elimination technique can be adopted for determining a univariate polynomial equation to solve.

In the following subsections, the closure-equation system will be deduced for both the cases.

### 3.1 Planar structure

Figure 2 shows the planar structure with the topology of Fig.1. With reference to Fig. 2,  $Q_i$  for  $i = 1, \dots, 4$ , are the points which locate the axes of the revolute pairs that join the quaternary link (link 0) to the  $i$ -th ternary link ( $i = 1, \dots, 4$ ).  $P_{ji}$  for  $j = 1, 2$ , and  $i = 1, \dots, 4$ , are the points that locate the axes of the revolute pairs that join the  $i$ -th ternary link to the two adjacent binary links.

Figure 3 shows the  $i$ -th loop ( $i = 1, \dots, 4$ ) of the PS, and the notation that will be used to deduce its loop equation. With reference to Fig. 3, the link-index  $k$  is equal to  $(i + 1)$  modulo 4.  $r_{0i}$  is the length of the segment  $\overline{Q_i Q_k}$ .  $r_{ji}$  ( $r_{jk}$ ),  $j = 1, 2$ , is the length of the segment  $\overline{Q_i P_{ji}}$  ( $\overline{Q_k P_{jk}}$ ). And  $r_{3(i+4)}$  is the length of the segment  $\overline{P_{2i} P_{1k}}$ . The angles  $\beta_i$ , and  $\gamma_i$  ( $\beta_k$ , and  $\gamma_k$ )

<sup>1</sup>The motion plane is a plane surface perpendicular to all the revolute pair axes.

<sup>2</sup>The unit sphere is a sphere surface with unit radius, and center coincident with the center of the spherical motion. It is worth noting that the unit sphere is perpendicular to all the revolute-pair axes since all the revolute-pair axes converge toward the center of the spherical motion.

<sup>3</sup>The distance between two points on a sphere surface is the length of the shortest great-circle arc joining the two points. On the unit sphere, this distance coincides with the convex central angle delimited by the two radii passing through the two points, if the angle is measured in radians.

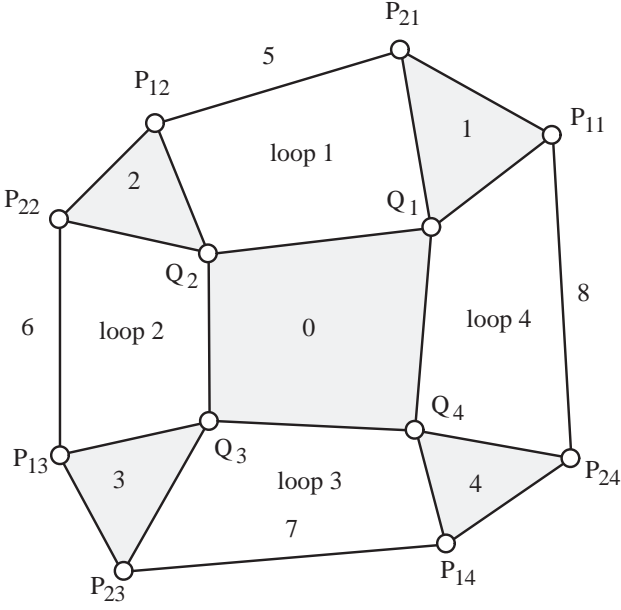


Figure 2: Four-loop PS with the topology of Fig. 1.

are the interior angles at  $Q_i$  ( $Q_k$ ) of link  $i$  (link  $k$ ) and link 0, respectively. The angle  $\theta_i$  ( $\theta_k$ ) is the joint variable of the revolute pair located by  $Q_i$  ( $Q_k$ ). Eventually, the reference system  $Q_i x_i y_i$  is a Cartesian reference system, fixed to link 0, that will be used to write the loop equation of the  $i$ -th loop.

It is worth noting that the eight geometric constants of the quaternary link (i.e.,  $\gamma_i$  and  $r_{0i}$  for  $i = 1, \dots, 4$ ) are related by the following three scalar equations (see Figs. 2 and 3):

$$\sum_{i=1}^4 \gamma_i = 2\pi \quad (1a)$$

$$r_{01} - r_{02} \cos \gamma_2 = r_{04} \cos \gamma_1 - r_{03} \cos(\gamma_1 + \gamma_4) \quad (1b)$$

$$r_{02} \sin \gamma_2 = r_{04} \sin \gamma_1 - r_{03} \sin(\gamma_1 + \gamma_4) \quad (1c)$$

With these notations, the position vectors of the points  $P_{2i}$  and  $P_{1k}$ , in the reference system  $Q_i x_i y_i$ , have the following explicit expressions ( $i = 1, \dots, 4; k = (i + 1) \text{ modulo } 4$ ):

$${}^i \mathbf{P}_{2i} = \begin{pmatrix} a_i c_i - b_i s_i \\ a_i s_i + b_i c_i \end{pmatrix}; \quad {}^i \mathbf{P}_{1k} = \begin{pmatrix} r_{1k} s_k \\ r_{0i} - r_{1k} c_k \end{pmatrix}; \quad (2)$$

where the left superscript  $i$  indicates that the vectors are measured in  $Q_i x_i y_i$ .  $c_i$  ( $c_k$ ), and  $s_i$  ( $s_k$ ) stand for  $\cos \theta_i$  ( $\cos \theta_k$ ), and  $\sin \theta_i$  ( $\sin \theta_k$ ), respectively. Eventually,  $a_i$  and  $b_i$  are geometric constants with the following explicit expressions:

$$a_i = r_{2i} \cos \left( \gamma_i + \beta_i - \frac{3}{2}\pi \right) \quad (3a)$$

$$b_i = r_{2i} \sin \left( \gamma_i + \beta_i - \frac{3}{2}\pi \right) \quad (3b)$$

By reminding that the distance  $r_{3(i+4)}$  between the points  $P_{2i}$  and  $P_{1k}$  (see Fig. 3) can be expressed through the coordinates of the two points, measured in any Cartesian reference system, the following set of closure equations can be written for the PS under study:

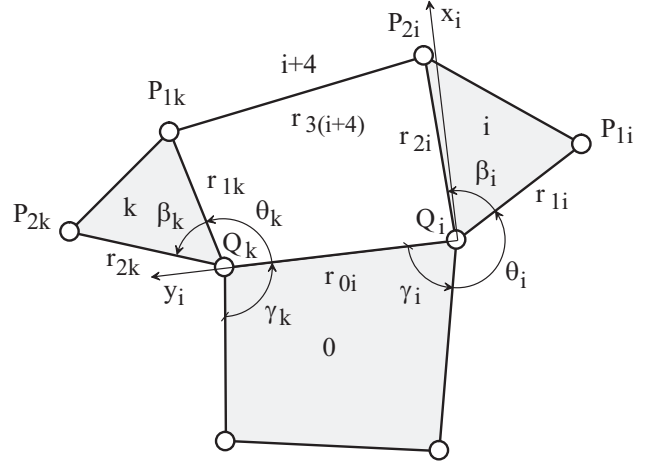


Figure 3:  $i$ -th loop of the PS: notation ( $i = 1, \dots, 4; k = (i + 1) \text{ modulo } 4$ ).

$$({}^i \mathbf{P}_{2i} - {}^i \mathbf{P}_{1k})^2 = r_{3(i+4)}^2, \quad (4)$$

$$i = 1, \dots, 4; k = (i + 1) \text{ modulo } 4.$$

The introduction of the explicit expressions (2) into Eqs. (4) yields the following system of closure equations in explicit form:

$$(a_i c_i - b_i s_i - r_{1k} s_k)^2 + (a_i s_i + b_i c_i - r_{0i} + r_{1k} c_k)^2 - r_{3(i+4)}^2 = 0, \quad (5)$$

$$i = 1, \dots, 4; k = (i + 1) \text{ modulo } 4.$$

Closure equations (5) constitute a system of four scalar equations in four unknowns: the four joint variables  $\theta_i$ ,  $i = 1, \dots, 4$ . By expanding (5), system (5) becomes:

$$g_{i0} + g_{i1} s_i + g_{i2} c_i + g_{i3} c_k + g_{i4} (s_i c_k - c_i s_k) + g_{i5} (c_i c_k + s_i s_k) = 0, \quad (6)$$

$$i = 1, \dots, 4; k = (i + 1) \text{ modulo } 4.$$

where the constant coefficients  $g_{in}$ ,  $n = 0, 1, \dots, 5$ , have the following explicit expressions:

$$g_{i0} = r_{2i}^2 + r_{1k}^2 + r_{0i}^2 - r_{3(i+4)}^2; \quad (7a)$$

$$g_{i1} = -2r_{0i} a_i; \quad g_{i2} = -2r_{0i} b_i; \quad g_{i3} = -2r_{0i} r_{1k}; \quad (7b)$$

$$g_{i4} = 2r_{1k} a_i; \quad g_{i5} = 2r_{1k} b_i. \quad (7c)$$

Each equation of system (6) is linear both in  $c_i$  and  $s_i$ , and in  $c_k$  and  $s_k$ .

### 3.2 Spherical structure

Figure 4 shows the spherical structure with the topology of Fig. 1. With reference to Fig. 4,  $O$  is the center of the unit sphere;  $Q_i$  for  $i = 1, \dots, 4$ , are the points which locate, on the unit sphere, the axes of the revolute pairs that join the quaternary link (link 0) to the  $i$ -th ternary link ( $i = 1, \dots, 4$ ).  $P_{ji}$  for  $j = 1, 2$ , and  $i = 1, \dots, 4$ , are the points that locate, on the unit sphere, the axes of the revolute pairs that join the  $i$ -th ternary link to the two adjacent binary links.

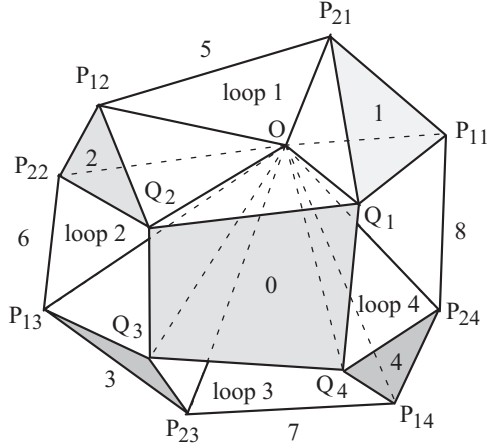


Figure 4: Four-loop SS with the topology of Fig. 1.

Figure 5 shows the  $i$ -th loop ( $i = 1, \dots, 4$ ) of the SS, and the notation that will be used to deduce its loop equation. With reference to Fig. 5, the link-index  $k$  is equal to  $(i + 1)$  modulo 4.  $\rho_{0i}$  is the convex central angle<sup>4</sup>  $\widehat{Q_i O Q_k}$ .  $\rho_{ji}$  ( $\rho_{jk}$ ),  $j = 1, 2$ , is the convex central angle  $\widehat{Q_i O P_{jk}}$  ( $\widehat{Q_k O P_{jk}}$ ). And  $\rho_{3(i+4)}$  is the convex central angle  $\widehat{P_{2i} O P_{1k}}$ . The angles  $\beta_i$ , and  $\gamma_i$  ( $\beta_k$ , and  $\gamma_k$ ) are the dihedral angles at the edge  $OQ_i$  ( $OQ_k$ ) of link  $i$  (link  $k$ ) and link 0, respectively. The angle  $\theta_i$  ( $\theta_k$ ) is the joint variable of the revolute pair located by  $Q_i$  ( $Q_k$ ). Eventually, the reference system  $Ox_i y_i z_i$  is a Cartesian reference system, fixed to link 0, that will be used to write the loop equation of the  $i$ -th loop.

It is worth noting that the eight geometric constants of the quaternary link (i.e.,  $\gamma_i$  and  $\rho_{0i}$  for  $i = 1, \dots, 4$ ) are related by any term of independent scalar equations deducible from the following matrix equation (see Figs. 4 and 5):

$${}^1\mathbf{R}_4 {}^4\mathbf{R}_3 {}^3\mathbf{R}_2 {}^2\mathbf{R}_1 = \mathbf{I} \quad (8)$$

where  $\mathbf{I}$  is the  $3 \times 3$  identity matrix; whereas  ${}^k\mathbf{R}_i$ ,  $k = (i + 1)$  modulo 4, is the rotation matrix that transforms vector components measured in  $Ox_i y_i z_i$  into vector components measured in  $Ox_k y_k z_k$ .  ${}^k\mathbf{R}_i$  has the following explicit expression:

$${}^k\mathbf{R}_i = \mathbf{R}_x(-\rho_{0i}) \mathbf{R}_z(\pi - \gamma_k) \quad (9)$$

where the following elementary rotation matrices have been introduced

$$\mathbf{R}_x(\alpha) = \begin{pmatrix} 1 & 0 & 0 \\ 0 & \cos \alpha & -\sin \alpha \\ 0 & \sin \alpha & \cos \alpha \end{pmatrix}; \quad (10a)$$

$$\mathbf{R}_z(\alpha) = \begin{pmatrix} \cos \alpha & -\sin \alpha & 0 \\ \sin \alpha & \cos \alpha & 0 \\ 0 & 0 & 1 \end{pmatrix}. \quad (10b)$$

<sup>4</sup>The measure of the convex central angle between two radius vectors gives the distance, on the unit sphere, between the two points located on the sphere by the two radius vectors.

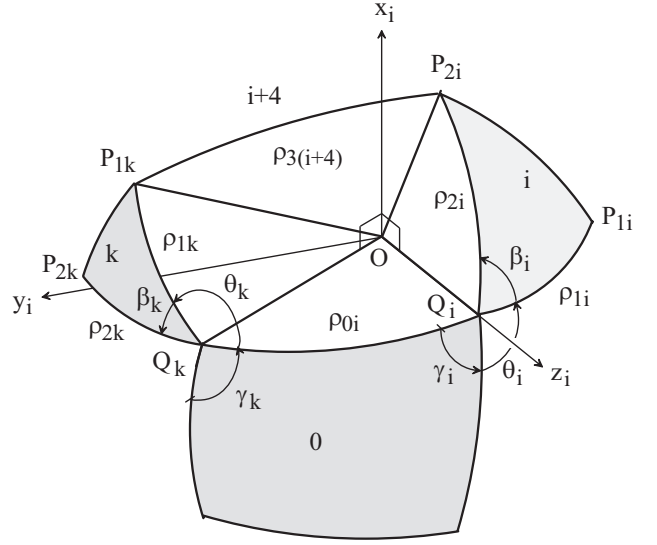


Figure 5:  $i$ -th loop of the SS: notation ( $i = 1, \dots, 4$ ;  $k = (i + 1)$  modulo 4).

With these notations, the position vectors of the points  $P_{2i}$  and  $P_{1k}$ , in the reference system  $Ox_i y_i z_i$ , have the following explicit expressions ( $i = 1, \dots, 4$ ;  $k = (i + 1)$  modulo 4):

$${}^i\mathbf{P}_{2i} = \begin{pmatrix} u_i c_i - v_i s_i \\ u_i s_i + v_i c_i \\ w_i \end{pmatrix}; \quad {}^i\mathbf{P}_{1k} = \begin{pmatrix} s_{1k} s_k \\ c_{1k} s_{0i} - s_{1k} c_{0i} c_k \\ c_{1k} c_{0i} + s_{1k} s_{0i} c_k \end{pmatrix}; \quad (11)$$

where the left superscript  $i$  indicates that the vectors are measured in  $Ox_i y_i z_i$ .  $c_i$  ( $c_k$ ), and  $s_i$  ( $s_k$ ) stand for  $\cos \theta_i$  ( $\cos \theta_k$ ), and  $\sin \theta_i$  ( $\sin \theta_k$ ), respectively; whereas  $c_{0i}$  ( $c_{1k}$ ), and  $s_{0i}$  ( $s_{1k}$ ) stand for  $\cos \rho_{0i}$  ( $\cos \rho_{1k}$ ), and  $\sin \rho_{0i}$  ( $\sin \rho_{1k}$ ), respectively. Eventually,  $u_i$ ,  $v_i$  and  $w_i$  are geometric constants with the following explicit expressions:

$$u_i = \sin \rho_{2i} \cos \left( \gamma_i + \beta_i - \frac{3}{2}\pi \right) \quad (12a)$$

$$v_i = \sin \rho_{2i} \sin \left( \gamma_i + \beta_i - \frac{3}{2}\pi \right) \quad (12b)$$

$$w_i = \cos \rho_{2i} \quad (12c)$$

Since  $\cos \rho_{3(i+4)}$  is equal to the dot product of the position vectors of the two unit-sphere points  $P_{2i}$  and  $P_{1k}$  (see Fig. 5) in any Cartesian reference system with origin at  $O$ ,<sup>5</sup> the following set of closure equations can be written for the SS under study:

$${}^i\mathbf{P}_{2i}^T {}^i\mathbf{P}_{1k} = c_{3(i+4)}, \quad i = 1, \dots, 4; k = (i+1) \text{ modulo } 4. \quad (13)$$

where  $c_{3(i+4)}$  stands for  $\cos \rho_{3(i+4)}$ , and the right superscript  $(\cdot)^T$  denotes the transpose of  $(\cdot)$ . The  $i$ -th equation (13) analytically expresses the fact that the distance, on the unit sphere, between the two unit-sphere points  $P_{2i}$  and  $P_{1k}$  is constant; hence, it is the spherical counterpart of the  $i$ -th equation (4).

<sup>5</sup>Remind that radius vectors of the unit sphere coincide with position vectors of the unit-sphere points, located by the radius vectors, in Cartesian reference systems with origin at the unit-sphere center  $O$ .

The introduction of the explicit expressions (11) into Eqs. (13) yields the following system of closure equations in explicit form:

$$\begin{aligned} & (u_i c_i - v_i s_i) s_{1k} s_k + \\ & (u_i s_i + v_i c_i) (c_{1k} s_{0i} - s_{1k} c_{0i} c_k) + \\ & w_i (c_{1k} c_{0i} + s_{1k} s_{0i} c_k) - c_{3(i+4)} = 0, \end{aligned} \quad (14)$$

$$i = 1, \dots, 4; k = (i + 1) \text{ modulo } 4.$$

Closure equations (14) constitute a system of four scalar equations in four unknowns: the four joint variables  $\theta_i$ ,  $i = 1, \dots, 4$ . By expanding (14), system (14) becomes:

$$\begin{aligned} & h_{i0} + h_{i1} s_i + h_{i2} c_i + h_{i3} c_k + \\ & h_{i4} s_i c_k + h_{i5} c_i s_k + h_{i6} c_i c_k + h_{i7} s_i s_k = 0, \end{aligned} \quad (15)$$

$$i = 1, \dots, 4; k = (i + 1) \text{ modulo } 4.$$

where the constant coefficients  $h_{in}$ ,  $n = 0, 1, \dots, 7$ , have the following explicit expressions:

$$h_{i0} = w_i c_{1k} c_{0i} - c_{3(i+4)}; \quad h_{i1} = u_i c_{1k} s_{0i}; \quad (16a)$$

$$h_{i2} = v_i c_{1k} s_{0i}; \quad h_{i3} = w_i s_{1k} s_{0i}; \quad h_{i4} = -u_i s_{1k} c_{0i}; \quad (16b)$$

$$h_{i5} = u_i s_{1k}; \quad h_{i6} = -v_i s_{1k} c_{0i}; \quad h_{i7} = -v_i s_{1k}. \quad (16c)$$

Each equation of system (15) is linear both in  $c_i$  and  $s_i$ , and in  $c_k$  and  $s_k$ .

#### 4 Solution technique

The closure-equation systems (6) and (15) can be transformed into algebraic-equation systems by using the following trigonometric identities:

$$c_i = \frac{1 - t_i^2}{1 + t_i^2}; \quad s_i = \frac{2t_i}{1 + t_i^2}; \quad i = 1, \dots, 4 \quad (17)$$

where  $t_i$ ,  $i = 1, \dots, 4$ , is equal to  $\tan(\theta_i/2)$ .

So doing, both system (6), and system (15) are put in the following form:

$$\sum_{n=0}^2 \sum_{m=0}^2 d_{inm} t_i^n t_k^m = 0; \quad i = 1, \dots, 4; k = (i + 1) \text{ modulo } 4 \quad (18)$$

where the explicit expressions of the constant coefficients  $d_{inm}$ ,  $n, m = 0, 1, 2$ , are reported in the appendices A and B for the PS and the SS, respectively.

The first ( $i = 1$ ) and the fourth ( $i = 4$ ) equations of system (18) can be rewritten in the following form:

$$A_2 t_1^2 + A_1 t_1 + A_0 = 0 \quad (19a)$$

$$B_2 t_1^2 + B_1 t_1 + B_0 = 0 \quad (19b)$$

where  $A_j = d_{1j2} t_2^2 + d_{1j1} t_2 + d_{1j0}$  and  $B_j = d_{42j} t_4^2 + d_{41j} t_4 + d_{40j}$ , for  $j = 0, 1, 2$ . Moreover, the second ( $i = 2$ ) and the third ( $i = 3$ ) equations of system (18) can be rewritten in the following form:

$$E_2 t_3^2 + E_1 t_3 + E_0 = 0 \quad (20a)$$

$$F_2 t_3^2 + F_1 t_3 + F_0 = 0 \quad (20b)$$

where  $E_j = d_{22j} t_2^2 + d_{21j} t_2 + d_{20j}$  and  $F_j = d_{3j2} t_4^2 + d_{3j1} t_4 + d_{3j0}$ , for  $j = 0, 1, 2$ .

The product of both the Eqs. (19) by  $t_1$  yields two more equations that, when added to (19), give the following homogeneous system:

$$\mathbf{M}_1 \mathbf{f}_1 = 0 \quad (21)$$

where  $\mathbf{f}_1$  is equal to  $(t_1^3, t_1^2, t_1, 1)^T$ , whereas  $\mathbf{M}_1$  is a  $4 \times 4$  matrix defined as follows

$$\mathbf{M}_1 = \begin{pmatrix} A_2 & A_1 & A_0 & 0 \\ B_2 & B_1 & B_0 & 0 \\ 0 & A_2 & A_1 & A_0 \\ 0 & B_2 & B_1 & B_0 \end{pmatrix} \quad (22)$$

On the other side, the product of both the Eqs. (20) by  $t_3$  yields two more equations that, when added to (20), give the following homogeneous system:

$$\mathbf{M}_2 \mathbf{f}_2 = 0 \quad (23)$$

where  $\mathbf{f}_2$  is equal to  $(t_3^3, t_3^2, t_3, 1)^T$ , whereas  $\mathbf{M}_2$  is a  $4 \times 4$  matrix defined as follows

$$\mathbf{M}_2 = \begin{pmatrix} E_2 & E_1 & E_0 & 0 \\ F_2 & F_1 & F_0 & 0 \\ 0 & E_2 & E_1 & E_0 \\ 0 & F_2 & F_1 & F_0 \end{pmatrix} \quad (24)$$

The two homogeneous systems (21) and (23) admit non-trivial solutions, for  $\mathbf{f}_1$  and  $\mathbf{f}_2$  respectively, if and only if the two determinants  $\det(\mathbf{M}_1)$  and  $\det(\mathbf{M}_2)$  are equal to zero (i.e., their coefficient matrices are singular). Since the entries of the first and the third rows of both the matrices are quadrics in  $t_2$ , whereas their second and fourth rows are quadrics in  $t_4$ , the vanishing condition of  $\det(\mathbf{M}_1)$  and  $\det(\mathbf{M}_2)$  yields the following two algebraic equations that are quartics both in  $t_2$  and in  $t_4$ :

$$\sum_{n=0}^4 \sum_{m=0}^4 p_{nm} t_2^n t_4^m = 0 \quad (25a)$$

$$\sum_{n=0}^4 \sum_{m=0}^4 q_{nm} t_2^n t_4^m = 0 \quad (25b)$$

where the explicit expressions of the constant coefficients  $p_{nm}$  and  $q_{nm}$ , for  $n, m = 0, \dots, 4$ , as functions of the constant coefficients reported in the appendices A and B, can be easily determined with the help of an algebraic manipulator. Such expressions are not reported here since they are cumbersome.

Equations (25) constitute a non-linear system of two equations in two unknowns:  $t_2$ , and  $t_4$ . System (25) can be rewritten as follows:

$$\sum_{j=0}^4 L_j t_2^j = 0 \quad (26a)$$

$$\sum_{j=0}^4 N_j t_2^j = 0 \quad (26b)$$

Table 1: Planar Structure: solutions of the numerical example

	$t_1$	$t_2$	$t_3$	$t_4$
1	.14540976407902879027293908	.64496623994571841596263372	-.33995155650823447070843769	.0819791126793446047065806293
2	-.077227714709025110370104775	.76803507980135176081753200	-.37583922874392176970779633	.0991483691462966418039440854
3	.31027317592256860100604449	-.78277181236408978593774468	.42188060295853963511347192	.2238289048835068617548207877
4	.45062695967325673049797405	-.69794362132646017838199605	-.97476498792723065506640091	.3378809249470220693696311392
5	1.20695305556324089196099633	.91633117401742338436255702	1.09130850106927139480659436	.8390996311772800117631272981
6	-.64640026596367343569314724	4.04003082965422103236594713	-2.71967984246300713821885292	1.045998408481253318241645595
7	1.66916735389394832010007919	1.14216132858181575837207037	1.37143762290017367135776656	1.050583466573429961237254444
8	13.16425818060947425215680863	4.26882828246928634814151261	-4.53789402060688689762408517	1.800982930765191163895773994
9	208.45038747133619402856213487	-2.11674168109901666421941153	-4.78562060550766382277121085	1.895978137292928399253752311
10	-26.81541066700656298137161586	-3.0776050900255959280955103	2.90357331147061231692162538	1.943292745104974910169838954
11	.039846847673210378188216602	-1.10048431924001936505603127	.55472513836233642331325649	-.084308385270921315258566334
12	-.15607071229759993578242963	-1.55698842971696026891592910	.78641617401213709094144928	-.167603233161461281813419201
13	.077971500241808447357197929	.67054918338255699388821957	.81579796381664550087115700	-.176970618142634298758693275
14	-.30820112784483839462288724	-2.22324243579987649268244828	1.25223538268247267422803279	-.302069667336494935593808144
15	-.32498273061036110891061454	1.09252930678734718250915716	1.30746020746642945930185019	-.316590516221194220495666284
16	1.7046575070945815221605462	.63770346854436767382116706	-.33797081342814258809109019	-.363773478707546671785525565
17	-.43210685728254645483179199	1.36268671107614166134072405	1.67488361163341613634156329	-.407984780649443848667174677
18	.52684373129210421002487735	-.66739051464043879792708220	-.93642359477505331961703787	-1.022462948427824666661923238
19	-32.55430091621347845561677664	-2.82792448537262388807377299	-253.73121491428977207738482685	-2.25282987723016144150037867
20	11.2505539957708095094706716	-1.47768067112559515995942455	-2.30168293097248032931051648	-2.42705297789839512570915480
21	10.87826714915480388273577657	3.85237293514646026565524521	-2.30523947165503596877276301	-2.43031231220896800404824993
22	10.59132861100362440506723393	3.79590172229500515671923849	-51.26410762602066041681539526	-2.4329321153224967522279903
23	-.46091396718-.3147647875 j	.92479484478+.6793627405 j	-.39930489512-.2398553778 j	-.44330155417-.2650496400 j
24	-.22634298550+.3044553268 j	-1.26354193430+.9102694686 j	-1.31998222381+1.436522544 j	.42996169345-.5607327793 j
25	-.27792212930+.2474597288 j	-1.51031256094+.9565297756 j	.65243761504-.4943832040 j	.50950215830-.4401832433 j
26	-.40592787199+.3396438907 j	.84446118451-.6023166102 j	.93036922244-.6829091211 j	.76616003143-.5562035841 j
27	-.40592787199-.3396438907 j	.84446118451+.6023166102 j	.93036922244+.6829091211 j	.76616003143+.5562035841 j
28	-.27792212930-.2474597288 j	-1.51031256094-.9565297756 j	.65243761504+.4943832040 j	.50950215830+.4401832433 j
29	-.22634298550-.3044553268 j	-1.26354193430-.9102694686 j	-1.31998222381-1.436522544 j	.42996169345+.5607327793 j
30	-.46091396718+.3147647875 j	.92479484478-.6793627405 j	-.39930489512+.2398553778 j	-.44330155417+.2650496400 j

where

$$L_j = \sum_{m=0}^4 p_{jm} t_4^m; N_j = \sum_{m=0}^4 q_{jm} t_4^m; j = 0, \dots, 4 \quad (27)$$

The product of both the Eqs. (26) by  $t_2, t_2^2$ , and  $t_2^3$  yields six more equations that, when added to (26), give the following homogeneous system:

$$\mathbf{H} \mathbf{e} = 0 \quad (28)$$

where  $\mathbf{e}$  is equal to  $(t_2^7, t_2^6, t_2^5, t_2^4, t_2^3, t_2^2, t_2, 1)^T$ , whereas  $\mathbf{H}$  is an  $8 \times 8$  matrix defined as follows

$$\mathbf{H} = \begin{pmatrix} L_4 & L_3 & L_2 & L_1 & L_0 & 0 & 0 & 0 \\ N_4 & N_3 & N_2 & N_1 & N_0 & 0 & 0 & 0 \\ 0 & L_4 & L_3 & L_2 & L_1 & L_0 & 0 & 0 \\ 0 & N_4 & N_3 & N_2 & N_1 & N_0 & 0 & 0 \\ 0 & 0 & L_4 & L_3 & L_2 & L_1 & L_0 & 0 \\ 0 & 0 & N_4 & N_3 & N_2 & N_1 & N_0 & 0 \\ 0 & 0 & 0 & L_4 & L_3 & L_2 & L_1 & L_0 \\ 0 & 0 & 0 & N_4 & N_3 & N_2 & N_1 & N_0 \end{pmatrix} \quad (29)$$

The homogeneous system (28) admits non-trivial solutions for  $\mathbf{e}$ , if and only if the following equation is satisfied:

$$\det(\mathbf{H}) = 0 \quad (30)$$

Since the non-null entries of matrix  $\mathbf{H}$  are univariate quartics in  $t_4$ , and  $\det(\mathbf{H})$  is a sum of terms that are products of eight entries of matrix  $\mathbf{H}$  (see Appendix C), Eq. (30) is a univariate polynomial equation in  $t_4$  which has at most degree 32.

This result meets the upper bound to the number of complex solutions of system (18) that the authors found by calculating the optimal multi-homogeneous Bézout number (see Malajovich *et al.* (2004); Wampler (1992) for details) of system (18). Once the values of  $t_4$  that solve Eq. (30) have been computed, by back substituting them into matrix  $\mathbf{H}$ , and, then, solving the resulting systems (28), the corresponding values of  $t_2$  can be computed. Eventually, the computed values of the couple  $\{t_2, t_4\}$  must be back substituted into (21) and (23) to compute the corresponding values of  $t_1$  and  $t_3$ .

The adopted elimination procedure could have introduced extraneous solutions of type  $\pm j$  with  $j = \sqrt{-1}$  since the only factors, that could generate extraneous roots and have been multiplied by the original system of equations, are the factors  $(1 + t_i^2)(1 + t_k^2)$ , with  $i = 1, \dots, 4$  and  $k = (i + 1)$  modulo 4. Such factors have been used to obtain system (18) from the original ones (i.e., either (6) or (15)) passing through the trigonometric identities (17).

So far, the evaluation of the actual degree of (30) can be done either through extended numerical tests, provided that they identify at least one set of data which makes (30) a 32-degree polynomial equation, or by analytically determining the coefficients of the polynomial equation (30).

Extended numerical tests, carried out by the authors, with randomly generated data brought to find many data sets, both for the planar geometry and for the spherical geometry, which make (30) a 32-degree polynomial equation. Moreover, the same numerical tests demonstrated that the elimination procedure used to obtain (30) introduces one couple of extraneous roots of type  $\pm j$

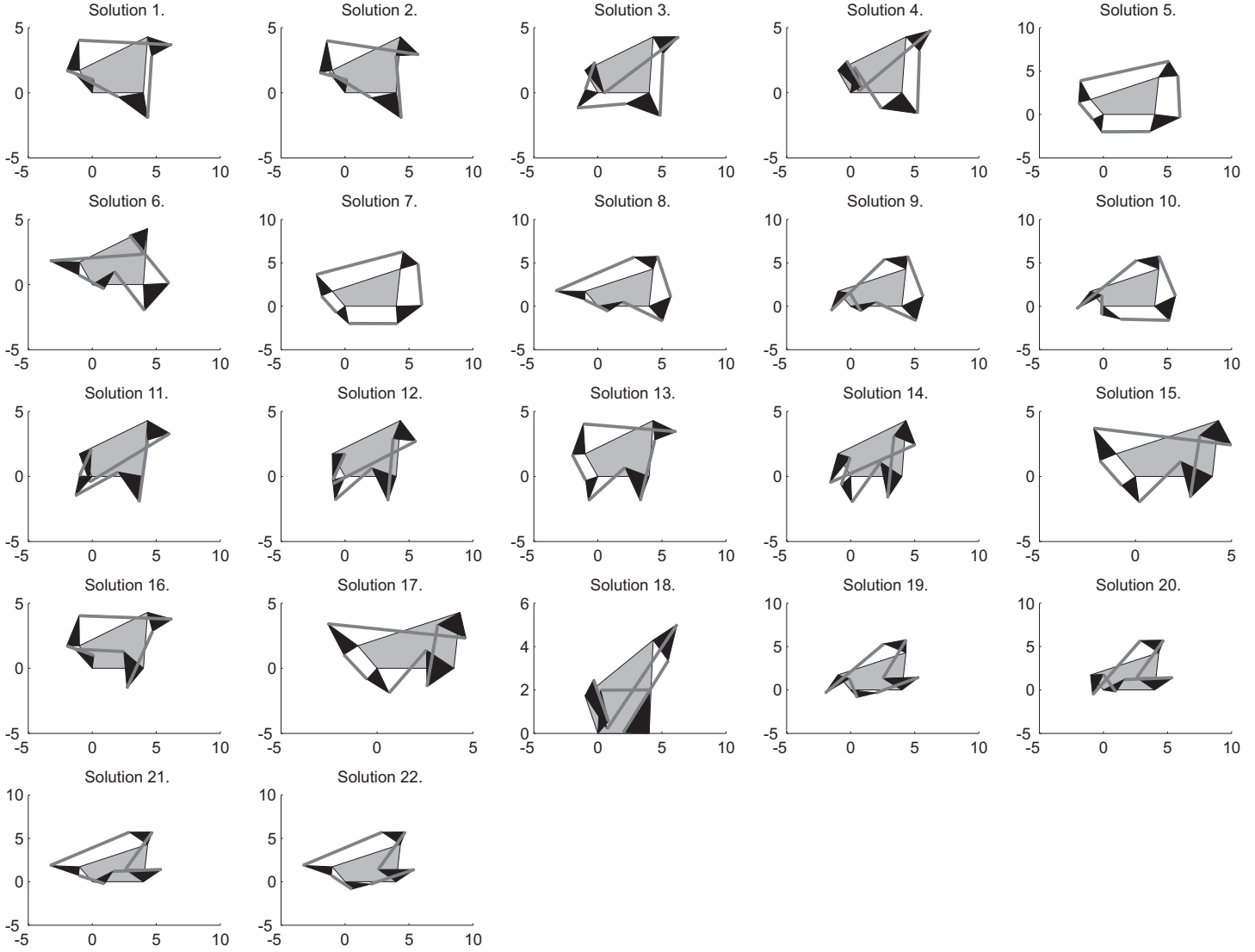


Figure 6: Assembly modes corresponding at the real solutions of the planar structure example,, numbered as in Table 1.

in the planar case, whereas does not introduce extraneous roots in the spherical case. These results bring to the conclusion that, in general, Eq. (30) is a 32-degree polynomial equation both for the planar geometry and for the spherical geometry, but, in the planar case, one common factor of type  $(1 + t_4^2)$  can always be collected and simplified. Thus, in general, the complex solutions of our problems are 30 for the planar case and 32 for the spherical case. Among the complex solutions of (18), only the real solutions correspond to actual assembly modes of the structure under study. The above-mentioned numerical tests brought to identify a PS geometry with 22 assembly modes and an SS geometry with 20 assembly modes. The maximum number of real solutions of Eq. (30) still is an open problem.

Regarding the analytic determination of the coefficients of the polynomial equation (30), it can be implemented with the help of an algebraic manipulator by, first, determining the explicit expression of  $\det(\mathbf{H})$  as a function of the non-null entries of matrix  $\mathbf{H}$  (see Appendix C), and, then, elaborating the obtained expression, either as a whole or by grouping terms according to the size

of the computer memory.

## 5 Numerical examples

Two numerical examples, one for the planar case and the other for the spherical case, are reported in this section in order to show the effectiveness of the proposed algorithm.

The algorithm has been implemented in Maple. The numerical computations have been executed by setting the machine precision equal to 32 decimal digits in Maple. All the computed solutions, when substituted into the closure equations, satisfy those equations with residuals whose absolute values range from less than  $10^{-24}$  to  $10^{-16}$  which is coherent with the chosen machine precision.

### 5.1 Planar structure

With reference to Fig. 3, the geometric data of the planar structure are (the angles are measured in radians; the lengths are mea-

Table 2: Spherical Structure: solutions of the numerical example

	$t_1$	$t_2$	$t_3$	$t_4$
1	.71210618362405426284256680	-1.07497455753610126844941610	-.44800329091214858293485363	.08888750399467942592826241
2	-.77555049530120851859608902	-.74503557530432738102964660	-.24792229123086817311120878	.10816694054981834932287101
3	.73108529113176738147778583	.36104413133812455092212669	-.23746745300156585250147610	.10950012413553095254398550
4	-.72549776292846969591003825	.79320769587113511335921109	.03630297251790967535735756	.16000844373201842754237919
5	-.63263922860470586533425186	-.56652126398478751309846081	-1.44902748818508054635389670	.27451592178874086050489859
6	1.57053701322224629303710825	-.52991180805252246579181921	-1.37210452664695894570979698	.68727090141199789465811756
7	2.40142765596175495890746839	.99959051861156910688335979	1.47191403359898321689225502	.99953905003138499326551774
8	2.94590500454578732727341691	1.14028145816754857419174148	1.68387120989711817340500497	1.14028145816754857419174148
9	-.32795607767030026969899765	2.19663385872870672116782892	3.92448007851295936217838809	2.44302088284558462087474599
10	-.35516231227752358582549022	-.28916074078427804669446380	-.94600220362422008355832889	3.26553951295171978376109941
11	-1.65975815407406043940241852	-2.56923193640685492125416214	9.79335321801512801048241709	5.03567470968899676965553945
12	-1.38917347319588278667302307	-1.84208964986328586214502214	-.84651594808033024796061489	5.61748994274721802111609339
13	.57581984213681238722225099	-1.30867847119402492580107470	-4.65455115661074888666990473	-.08542804448235159783879797
14	-1.04104284673259602904066614	-1.14747508391672336044297166	-3.50406969845887886005942853	-.10012284021138216272481265
15	-1.61463716957538962922155030	.24467583838696498764648277	.54597642903231132114054648	-.36991906499149841363008628
16	.42332462997183013284378318	.20417982508098921066693455	.50514822416316912555231635	-.39495622231747702816149454
17	-2.62820087281999567358612281	-9.29741813777522859855414691	-2.57059162668172064761692181	-.61864963851011157573145133
18	.55460724172756564825008630	.27238511180213352674820919	-.30818076970875067831990899	-2.21676044670613406595744070
19	.59483291307175496023888520	-1.26993077235092135957743913	-4.33353238096872539657203809	-2.25993333485671694287174695
20	.90142516808676214346285897	-.86488448942789661222868463	-.32303829136494826043861252	-2.31799366029688446938212761
21	.00342194452 -1.44883692156 j	-.07299074451 -1.36795252833 j	-.56722944684 -1.42617220241 j	-.57746797303 -2.18365466581 j
22	.00342194452 +1.44883692156 j	-.07299074451 +1.36795252833 j	-.56722944684 +1.42617220241 j	-.57746797303 +2.18365466581 j
23	.07455997783 -1.12122912972 j	-3.11221184246 -3.63391279861 j	-1.81717583594 -1.05093035245 j	-.27842265152 -1.15434019112 j
24	.07455997783 +1.12122912972 j	-3.11221184246 +3.63391279861 j	-1.81717583594 +1.05093035245 j	-.27842265152 +1.15434019112 j
25	-.23381078635 -1.21762411406 j	.09063269535 -1.17945847211 j	.04271862463 -1.73206889984 j	-.21193805682 -1.94629004473 j
26	-.23381078635 +1.21762411406 j	.09063269535 +1.17945847211 j	.04271862463 +1.73206889984 j	-.21193805682 +1.94629004473 j
27	-.55234273464 -1.64624481380 j	.14522125200 -1.66631164661 j	.32805303569 -1.64275586423 j	-.03952558872 -1.56289938664 j
28	-.55234273464 +1.64624481380 j	.14522125200 +1.66631164661 j	.32805303569 +1.64275586423 j	-.03952558872 +1.56289938664 j
29	.09011189540 -1.15046250591 j	.10893422241 -1.97670327545 j	.15179864121 -1.99221796677 j	.07761152840 -1.02215361384 j
30	.09011189540 +1.15046250591 j	.10893422241 +1.97670327545 j	.15179864121 +1.99221796677 j	.07761152840 +1.02215361384 j
31	-.13337931843 -1.39981317759 j	.27358440193 -1.79147591705 j	.32398368945 -1.86102638956 j	.12386266728 -1.81145941293 j
32	-.13337931843 +1.39981317759 j	.27358440193 +1.79147591705 j	.32398368945 +1.86102638956 j	.12386266728 +1.81145941293 j

sured in a generic unit of length):

$$\begin{aligned}
\gamma_1 &= \pi/3 & \gamma_2 &= 10\pi/21 & \gamma_3 &= 2\pi/3 & \gamma_4 &= 11\pi/21 \\
\beta_1 &= \pi/3 & \beta_2 &= \pi/2 & \beta_3 &= 5\pi/18 & \beta_4 &= \pi/2 \\
r_{11} &= 1.5 & r_{12} &= 2.3 & r_{13} &= 1 & r_{14} &= 2 \\
r_{21} &= 2 & r_{22} &= 1 & r_{23} &= 2 & r_{24} &= 2 \\
r_{01} &= 5.9068 & r_{02} &= 2 & r_{03} &= 4 & r_{04} &= 4.3069 \\
r_{35} &= 7.2893 & r_{36} &= 2.2485 & r_{37} &= 3.8270 & r_{38} &= 4.8127
\end{aligned}$$

Among these geometric data, the parameters  $\gamma_4$ ,  $r_{01}$  and  $r_{04}$  have been computed by using relationships (1) together with the values of the other geometric data of the quaternary link. Moreover, once the geometry of the quaternary and the ternary links were defined, the lengths of the binary links (i.e.,  $r_{35}$ ,  $r_{36}$ ,  $r_{37}$ , and  $r_{38}$ ) have been computed through Eqs. (4) after the following values of the angles  $\theta_i$ ,  $i = 1, \dots, 4$ , were assigned:

$$\theta_1 = 47\pi/84 \quad \theta_2 = 17\pi/36 \quad \theta_3 = 19\pi/36 \quad \theta_4 = 4\pi/9,$$

which correspond to ( $t_i = \tan(\theta_i/2)$ )

$$\begin{aligned}
t_1 &= 1.2069530555 & t_2 &= 0.9163311740 \\
t_3 &= 1.0913085010 & t_4 &= 0.8390996311
\end{aligned}$$

This reference assembly mode appears in table 1 as solution number 5.

All the computed solutions of system (18) for this planar geometry are reported in table 1. Among the 30 solutions reported in table 1, the first 22 solutions are real. Therefore the studied planar geometry admits 22 assembly modes that are schemed in Fig.6.

## 5.2 Spherical structure

With reference to Fig. 5, the geometric data of the spherical structure are (the angles are measured in radians):

$$\begin{aligned}
\gamma_1 &= \pi/6 & \gamma_2 &= 2\pi/3 & \gamma_3 &= 1.62440 & \gamma_4 &= 2\pi/3 \\
\beta_1 &= \pi/4 & \beta_2 &= \pi/4 & \beta_3 &= \pi/6 & \beta_4 &= \pi/4 \\
\rho_{11} &= \pi/5 & \rho_{12} &= \pi/7 & \rho_{13} &= \pi/5 & \rho_{14} &= \pi/6 \\
\rho_{21} &= \pi/5 & \rho_{22} &= \pi/7 & \rho_{23} &= \pi/5 & \rho_{24} &= \pi/6 \\
\rho_{01} &= 0.1855 & \rho_{02} &= 0.1068 & \rho_{03} &= \pi/7 & \rho_{04} &= \pi/8 \\
\rho_{35} &= 0.7099 & \rho_{36} &= 0.4532 & \rho_{37} &= 0.7324 & \rho_{38} &= 0.8997
\end{aligned}$$

Among these geometric data, the angles  $\rho_{01}$ ,  $\rho_{02}$  and  $\gamma_3$  have been computed by using a tern of independent scalar equations, deduced from the matrix Eq. (8), together with the values of the other geometric data of the quaternary link. Moreover, once the geometry of the quaternary and the ternary links were defined, the central angles of the binary links (i.e.,  $\rho_{35}$ ,  $\rho_{36}$ ,  $\rho_{37}$ , and  $\rho_{38}$ ) have been computed through Eqs. (13) after the following values of the angles  $\theta_i$ ,  $i = 1, \dots, 4$ , were assigned:

$$\begin{aligned}
\theta_1 &= 19\pi/24 & \theta_2 &= 13\pi/24 \\
\theta_3 &= (11\pi/12) - (81/100) & \theta_4 &= 13\pi/24
\end{aligned}$$

which correspond to ( $t_i = \tan(\theta_i/2)$ )

$$\begin{aligned}
t_1 &= 2.945905004545 & t_2 &= 1.140281458167 \\
t_3 &= 1.683871209897 & t_4 &= 1.140281458167
\end{aligned}$$

This reference assembly mode appears in table 2 as solution number 8.

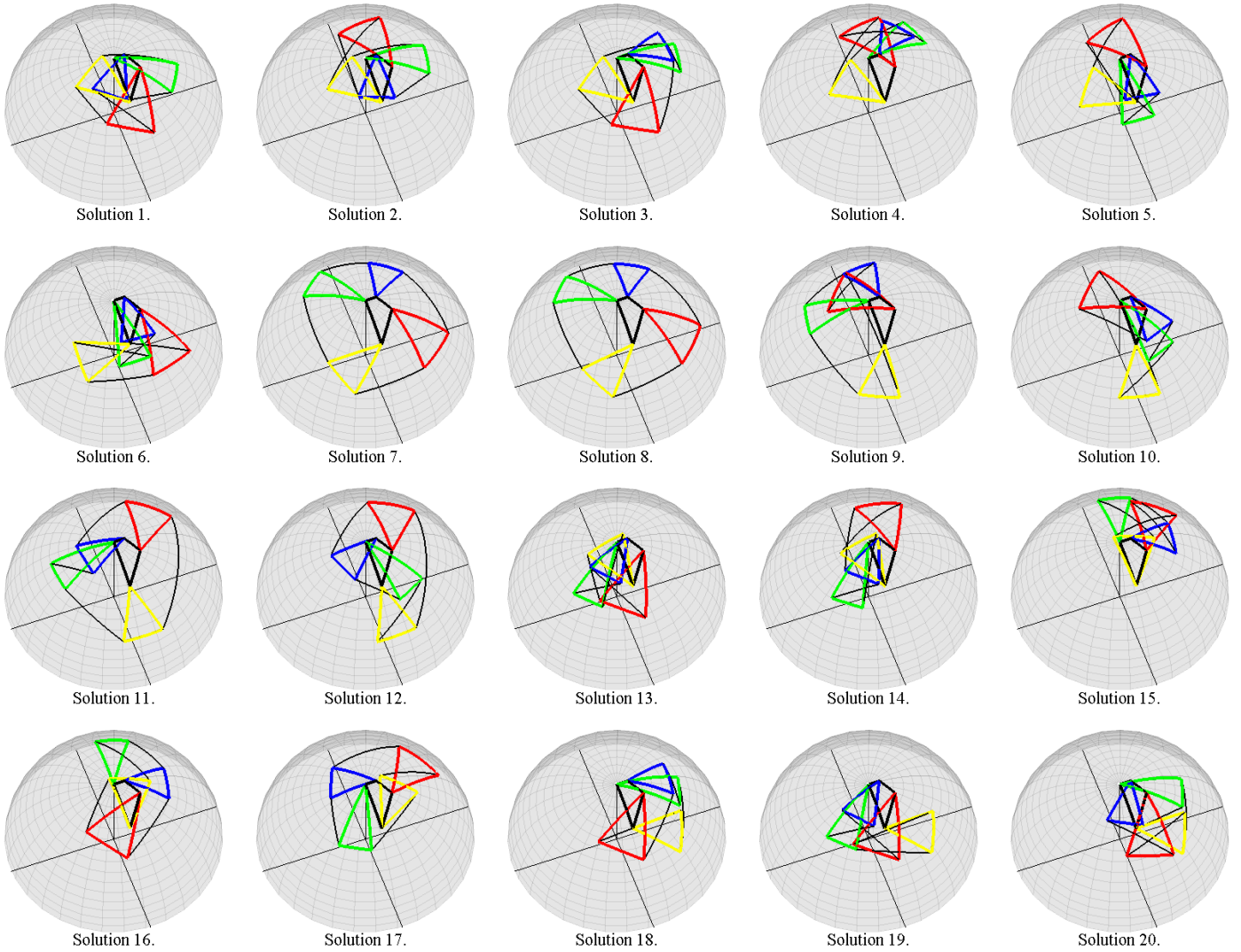


Figure 7: Assembly modes corresponding at the real solutions of the spherical structure example, numbered as in Table 2.

All the computed solutions of system (18) for this spherical geometry are reported in table 2. Among the 32 solutions reported in table 2, the first 20 solutions are real. Therefore the studied spherical geometry admits 20 assembly modes schemed in Fig.7.

## 6 Conclusions and further research

An algorithm that determines all the assembly modes of two structures with the same topology has been presented.

The topology of the studied structures is constituted of nine links (one quaternary link, four ternary links and four binary links) connected through twelve revolute pairs to form four closed loops.

Such structures can be thought as generated from two large families (one planar and the other spherical) of parallel manipulators by locking the actuated joints. Thus, the proposed algorithm can be used to solve the direct position analysis (DPA) of

all these manipulators.

Through the proposed algorithm, it has been demonstrated that the DPA of the planar manipulators with this topology has thirty complex solutions, whereas the DPA of their spherical counterparts has thirty-two complex solutions. Moreover, extended numerical tests, which used the proposed algorithm, brought to find a planar geometry with 22 assembly modes (i.e.,real solutions of the DPA) and a spherical geometry with 20 assembly modes, and demonstrated the robustness of the algorithm. As far as the authors are aware, these results are new.

This work is framed into a research activity oriented to provide algorithms that solve the DPA of all the planar and spherical parallel manipulators which become four-loop Assur kinematic chains when their actuators are locked.

In the future, the studied architectures will be used to synthesize devices for industrial and/or biomedical applications.

## Acknowledgment

This work has been partially supported by the Spanish Ministry of Education and Science, under the I+D project DPI2007-60858, by the I3P program with a short stay grant, and by funds of the Italian MIUR.

## References

- C. Innocenti, "Polynomial solution to the position analysis of the 7-link Assur kinematic chain with one quaternary link", *Mechanism and Machine Theory*, Vol. 30, pp. 1295-1303, 1995.
- G. Malajovich, and K. Meer, "Computing multi-homogeneous Bézout numbers is hard", Preprint, <http://www.arxiv.org/abs/cs/0405021>, 2004.
- N.I. Manolescu, "A method based on Baranov trusses, and using graph theory to find the set of planar jointed kinematic chains and mechanisms", *Mechanism and Machine Theory*, Vol. 8, pp. 3-22, 1973.
- H. Shen, K.-L. Ting, T.-L. Yang, "Configuration analysis of complex multiloop linkages and manipulators", *Mechanism and Machine Theory*, Vol. 35, pp. 353-362, 2000.
- C.W. Wampler, "Bézout number calculations for multi-homogeneous Polynomial Systems", *Applied mathematics and computation*, Vol. 51, pp.143-157, 1992.
- C.W. Wampler, "Displacement analysis of spherical mechanisms having three or fewer loops", *Journal of Mechanical Design*, Vol. 126, pp. 93-100, 2004.

## Appendix A

With reference to (18) and (7), the constant coefficients  $d_{inm}$ ,  $n, m = 0, 1, 2$ , have the following explicit expressions for the planar structure (Fig. 2):

$$\begin{aligned} d_{i00} &= g_{i0} + g_{i2} + g_{i3} + g_{i5}; & d_{i10} &= 2(g_{i1} + g_{i4}); \\ d_{i01} &= -2g_{i4}; & d_{i11} &= 4g_{i5}; & d_{i20} &= g_{i0} - g_{i2} + g_{i3} - g_{i5}; \\ d_{i02} &= g_{i0} + g_{i2} - g_{i3} - g_{i5}; & d_{i12} &= 2(g_{i1} - g_{i4}); \\ d_{i21} &= 2g_{i4}; & d_{i22} &= g_{i0} - g_{i2} - g_{i3} + g_{i5}. \end{aligned}$$

## Appendix B

With reference to (18) and (16), the constant coefficients  $d_{inm}$ ,  $n, m = 0, 1, 2$ , have the following explicit expressions for the spherical structure (Fig. 4):

$$\begin{aligned} d_{i00} &= h_{i0} + h_{i2} + h_{i3} + h_{i6}; & d_{i10} &= 2(h_{i1} + h_{i4}); \\ d_{i01} &= 2h_{i5}; & d_{i11} &= 4h_{i7}; & d_{i20} &= h_{i0} - h_{i2} + h_{i3} - h_{i6}; \\ d_{i02} &= h_{i0} + h_{i2} - h_{i3} - h_{i6}; & d_{i12} &= 2(h_{i1} - h_{i4}); \\ d_{i21} &= -2h_{i5}; & d_{i22} &= h_{i0} - h_{i2} - h_{i3} + h_{i6}. \end{aligned}$$

## Appendix C

The explicit expression of  $\det(\mathbf{H})$  as a function of the non-null entries of matrix  $\mathbf{H}$  (see definition (29)) is:

$$\begin{aligned} \det(\mathbf{H}) &= L_4^4 N_0^4 - L_3 L_4^3 N_0^3 N_1 + L_2 L_4^3 N_0^2 N_1^2 - \\ &L_1 L_4^3 N_0 N_1^3 + L_0 L_4^3 N_1^4 + L_3^2 L_4^2 N_0^2 N_2 - 2L_2 L_4^3 N_0^3 N_2 - \\ &L_2 L_3 L_4^2 N_0^2 N_1 N_2 + 3L_1 L_4^3 N_0^2 N_1 N_2 + L_1 L_3 L_4^2 N_0 N_1^2 N_2 - \\ &4L_0 L_4^3 N_0 N_1^2 N_2 - L_0 L_3 L_4^2 N_1^3 N_2 + L_2^2 L_4^2 N_0^2 N_2^2 - \\ &2L_1 L_3 L_4^2 N_0^2 N_2^2 + 2L_0 L_4^3 N_0^2 N_2^2 - L_1 L_2 L_4^2 N_0 N_1 N_2^2 + \\ &3L_0 L_3 L_4^2 N_0 N_1 N_2^2 + L_0 L_2 L_4^2 N_1^2 N_2^2 + L_1^2 L_4^2 N_0 N_2^3 - \\ &2L_0 L_2 L_4^2 N_0 N_2^3 - L_0 L_1 L_4^2 N_1 N_2^3 + L_0^2 L_4^2 N_2^4 - L_3^2 L_4 N_0^3 N_3 + \\ &3L_2 L_3 L_4^2 N_0^3 N_3 - 3L_1 L_4^3 N_0^3 N_3 + L_2 L_3^2 L_4 N_0^2 N_1 N_3 - \\ &2L_2^2 L_4^2 N_0^2 N_1 N_3 - L_1 L_3 L_4^2 N_0^2 N_1 N_3 + 4L_0 L_4^3 N_0^2 N_1 N_3 - \\ &L_1 L_3^2 L_4 N_0 N_1^2 N_3 + 2L_1 L_2 L_4^2 N_0 N_1^2 N_3 + L_0 L_3 L_4^2 N_0 N_1^2 N_3 + \\ &L_0 L_3^2 L_4 N_1^3 N_3 - 2L_0 L_2 L_4^2 N_1^3 N_3 - L_2^2 L_3 L_4 N_0^2 N_2 N_3 + \\ &2L_1 L_3^2 L_4 N_0^2 N_2 N_3 + L_1 L_2 L_4^2 N_0^2 N_2 N_3 - 5L_0 L_3 L_4^2 N_0^2 N_2 N_3 + \\ &L_1 L_2 L_3 L_4 N_0 N_1 N_2 N_3 - 3L_0 L_3^2 L_4 N_0 N_1 N_2 N_3 - \\ &3L_2^2 L_4^2 N_0 N_1 N_2 N_3 + 4L_0 L_2 L_4^2 N_0 N_1 N_2 N_3 - \\ &L_0 L_2 L_3 L_4 N_1^2 N_2 N_3 + 3L_0 L_1 L_4^2 N_1^2 N_2 N_3 - \\ &L_2^2 L_3 L_4 N_0 N_2^2 N_3 + 2L_0 L_2 L_3 L_4 N_0 N_2^2 N_3 + L_0 L_1 L_4^2 N_0 N_2^2 N_3 + \\ &L_0 L_1 L_3 L_4 N_1 N_2^2 N_3 - 4L_0^2 L_4^2 N_1 N_2^2 N_3 - L_0^2 L_3 L_4 N_2^3 N_3 + \\ &L_2^2 L_4 N_0^2 N_3^2 - 3L_1 L_2 L_3 L_4 N_0^2 N_3^2 + 3L_0 L_3^2 L_4 N_0^2 N_3^2 + \\ &3L_2^2 L_4^2 N_0^2 N_3^2 - 3L_0 L_2 L_4^2 N_0^2 N_3^2 - L_1 L_2^2 L_4 N_0 N_1 N_3^2 + \\ &2L_2^2 L_3 L_4 N_0 N_1 N_3^2 + L_0 L_2 L_3 L_4 N_0 N_1 N_3^2 - \\ &5L_0 L_1 L_4^2 N_0 N_1 N_3^2 + L_0 L_2^2 L_4 N_1^2 N_3^2 - 2L_0 L_1 L_3 L_4 N_1^2 N_3^2 + \\ &2L_2^2 L_4^2 N_1^2 N_3^2 + L_1^2 L_2 L_4 N_0 N_2 N_3^2 - 2L_0 L_2^2 L_4 N_0 N_2 N_3^2 - \\ &L_0 L_1 L_3 L_4 N_0 N_2 N_3^2 + 4L_0^2 L_4^2 N_0 N_2 N_3^2 - L_0 L_1 L_2 L_4 N_1 N_2 N_3^2 + \\ &3L_0^2 L_3 L_4 N_1 N_2 N_3^2 + L_0^2 L_2 L_4 N_2^2 N_3^2 - L_3^3 L_4 N_0 N_3^3 + \\ &3L_0 L_1 L_2 L_4 N_0 N_3^3 - 3L_0^2 L_3 L_4 N_0 N_3^3 + L_0 L_1^2 L_4 N_1 N_3^3 - \\ &2L_0^2 L_2 L_4 N_1 N_3^3 - L_0^2 L_1 L_4 N_2 N_3^3 + L_0^3 L_4 N_3^4 + L_4^3 N_0^3 N_4 - \\ &4L_2 L_3^2 L_4 N_0^3 N_4 + 2L_2^2 L_4^2 N_0^3 N_4 + 4L_1 L_3 L_4^2 N_0^3 N_4 - \\ &4L_0 L_4^3 N_0^3 N_4 - L_2 L_3^3 N_0^2 N_1 N_4 + 3L_2^2 L_3 L_4 N_0^2 N_1 N_4 + \\ &L_1 L_3^2 L_4 N_0^2 N_1 N_4 - 5L_1 L_2 L_4^2 N_0^2 N_1 N_4 - L_0 L_3 L_4^2 N_0^2 N_1 N_4 + \\ &L_1 L_3^3 N_0 N_1^2 N_4 - 3L_1 L_2 L_3 L_4 N_0 N_1^2 N_4 - L_0 L_3^2 L_4 N_0 N_1^2 N_4 + \\ &3L_2^2 L_4^2 N_0 N_1^2 N_4 + 2L_0 L_2 L_4^2 N_0 N_1^2 N_4 - L_0 L_3^3 N_1^3 N_4 + \\ &3L_0 L_2 L_3 L_4 N_1^3 N_4 - 3L_0 L_1 L_4^2 N_1^3 N_4 + L_2^2 L_3^2 N_0^2 N_2 N_4 - \\ &2L_1 L_3^3 N_0^2 N_2 N_4 - 2L_2^2 L_4 N_0^2 N_2 N_4 + 4L_1 L_2 L_3 L_4 N_0^2 N_2 N_4 + \\ &2L_0 L_3^2 L_4 N_0^2 N_2 N_4 - 3L_1^2 L_4^2 N_0^2 N_2 N_4 + 2L_0 L_2 L_4^2 N_0^2 N_2 N_4 - \\ &L_1 L_2 L_3^2 N_0 N_1 N_2 N_4 + 3L_0 L_3^3 N_0 N_1 N_2 N_4 + \\ &2L_1 L_2^2 L_4 N_0 N_1 N_2 N_4 + L_1^2 L_3 L_4 N_0 N_1 N_2 N_4 - \\ &8L_0 L_2 L_3 L_4 N_0 N_1 N_2 N_4 + 2L_0 L_1 L_4^2 N_0 N_1 N_2 N_4 + \\ &L_0 L_2 L_3^2 N_1^2 N_2 N_4 - 2L_0 L_2^2 L_4 N_1^2 N_2 N_4 - L_0 L_1 L_3 L_4 N_1^2 N_2 N_4 + \\ &4L_0^2 L_4^2 N_1^2 N_2 N_4 + L_1^2 L_3^2 N_0 N_2^2 N_4 - 2L_0 L_2 L_3^2 N_0 N_2^2 N_4 - \\ &2L_2^2 L_2 L_4 N_0 N_2^2 N_4 + 4L_0 L_2^2 L_4 N_0 N_2^2 N_4 - 4L_0^2 L_4^2 N_0 N_2^2 N_4 - \\ &L_0 L_1 L_3^2 N_1 N_2^2 N_4 + 2L_0 L_1 L_2 L_4 N_1 N_2^2 N_4 + L_0^2 L_3 L_4 N_1 N_2^2 N_4 + \\ &L_0^2 L_3^2 N_2^3 N_4 - 2L_0^2 L_2 L_4 N_2^3 N_4 - L_3^2 L_3 N_0^2 N_3 N_4 + \\ &3L_1 L_2 L_3^2 N_0^2 N_3 N_4 - 3L_0 L_3^3 N_0^2 N_3 N_4 + L_1 L_2^2 L_4 N_0^2 N_3 N_4 - \\ &5L_1^2 L_3 L_4 N_0^2 N_3 N_4 + 2L_0 L_2 L_3 L_4 N_0^2 N_3 N_4 + \\ &5L_0 L_1 L_4^2 N_0^2 N_3 N_4 + L_1 L_2^2 L_3 N_0 N_1 N_3 N_4 - \\ &2L_1^2 L_3^2 N_0 N_1 N_3 N_4 - L_0 L_2 L_3^2 N_0 N_1 N_3 N_4 - \\ &L_2^2 L_2 L_4 N_0 N_1 N_3 N_4 + 10L_0 L_1 L_3 L_4 N_0 N_1 N_3 N_4 - \\ &8L_0^2 L_4^2 N_0 N_1 N_3 N_4 - L_0 L_2^2 L_3 N_1^2 N_3 N_4 + 2L_0 L_1 L_3^2 N_1^2 N_3 N_4 + \\ &L_0 L_1 L_2 L_4 N_1^2 N_3 N_4 - 5L_0^2 L_3 L_4 N_1^2 N_3 N_4 - \\ &L_2^2 L_2 L_3 N_0 N_2 N_3 N_4 + 2L_0 L_2^2 L_3 N_0 N_2 N_3 N_4 + \\ &L_0 L_1 L_3^2 N_0 N_2 N_3 N_4 + 3L_1^3 L_4 N_0 N_2 N_3 N_4 - \\ &8L_0 L_1 L_2 L_4 N_0 N_2 N_3 N_4 + 2L_0^2 L_3 L_4 N_0 N_2 N_3 N_4 + \\ &L_0 L_1 L_2 L_3 N_1 N_2 N_3 N_4 - 3L_0^2 L_3^2 N_1 N_2 N_3 N_4 - \end{aligned}$$

$$\begin{aligned}
& 3L_0L_1^2L_4N_1N_2N_3N_4 + 4L_0^2L_2L_4N_1N_2N_3N_4 - \\
& L_0^2L_2L_3N_2^2N_3N_4 + 3L_0^2L_1L_4N_2^2N_3N_4 + L_1^3L_3N_0N_3^2N_4 - \\
& 3L_0L_1L_2L_3N_0N_3^2N_4 + 3L_0^2L_3^2N_0N_3^2N_4 - L_0L_1^2L_4N_0N_3^2N_4 + \\
& 2L_0^2L_2L_4N_0N_3^2N_4 - L_0L_1^2L_3N_1N_3^2N_4 + 2L_0^2L_2L_3N_1N_3^2N_4 + \\
& L_0^2L_1L_4N_1N_3^2N_4 + L_0^2L_1L_3N_2N_3^2N_4 - 4L_0^3L_4N_2N_3^2N_4 - \\
& L_0^3L_3N_3^2N_4 + L_2^4N_0^2N_4^2 - 4L_1L_2^2L_3N_0^2N_4^2 + 2L_1^2L_3^2N_0^2N_4^2 + \\
& 4L_0L_2L_3^2N_0^2N_4^2 + 4L_1^2L_2L_4N_0^2N_4^2 - 4L_0L_2^2L_4N_0^2N_4^2 - \\
& 8L_0L_1L_3L_4N_0^2N_4^2 + 6L_0^2L_4^2N_0^2N_4^2 - L_1L_2^3N_0N_1N_4^2 + \\
& 3L_1^2L_2L_3N_0N_1N_4^2 + L_0L_2^2L_3N_0N_1N_4^2 - 5L_0L_1L_3^2N_0N_1N_4^2 - \\
& 3L_1^3L_4N_0N_1N_4^2 + 2L_0L_1L_2L_4N_0N_1N_4^2 + 5L_0^2L_3L_4N_0N_1N_4^2 + \\
& L_0L_3^2N_1^2N_4^2 - 3L_0L_1L_2L_3N_1^2N_4^2 + 3L_0^2L_3^2N_1^2N_4^2 + \\
& 3L_0L_1^2L_4N_1^2N_4^2 - 3L_0^2L_2L_4N_1^2N_4^2 + L_1^2L_2^2N_0N_2N_4^2 - \\
& 2L_0L_3^2N_0N_2N_4^2 - 2L_1^3L_3N_0N_2N_4^2 + 4L_0L_1L_2L_3N_0N_2N_4^2 - \\
& 3L_0^2L_3^2N_0N_2N_4^2 + 2L_0L_1^2L_4N_0N_2N_4^2 + 2L_0^2L_2L_4N_0N_2N_4^2 - \\
& L_0L_1L_2^2N_1N_2N_4^2 + 2L_0L_1^2L_3N_1N_2N_4^2 + L_0^2L_2L_3N_1N_2N_4^2 - \\
& 5L_0^2L_1L_4N_1N_2N_4^2 + L_0^2L_2^2N_2^2N_4^2 - 2L_0^2L_1L_3N_2^2N_4^2 + \\
& 2L_0^3L_4N_2^2N_4^2 - L_1^3L_2N_0N_3N_4^2 + 3L_0L_1L_2^2N_0N_3N_4^2 + \\
& L_0L_1^2L_3N_0N_3N_4^2 - 5L_0^2L_2L_3N_0N_3N_4^2 - L_0^2L_1L_4N_0N_3N_4^2 + \\
& L_0L_1^2L_2N_1N_3N_4^2 - 2L_0^2L_2^2N_1N_3N_4^2 - L_0^2L_1L_3N_1N_3N_4^2 + \\
& 4L_0^3L_4N_1N_3N_4^2 - L_0^2L_1L_2N_2N_3N_4^2 + 3L_0^3L_3N_2N_3N_4^2 + \\
& L_0^3L_2N_3^2N_4^2 + L_1^4N_0N_4^3 - 4L_0L_1^2L_2N_0N_4^3 + 2L_0^2L_2^2N_0N_4^3 + \\
& 4L_0^2L_1L_3N_0N_4^3 - 4L_0^3L_4N_0N_4^3 - L_0L_1^3N_1N_4^3 + \\
& 3L_0^2L_1L_2N_1N_4^3 - 3L_0^3L_3N_1N_4^3 + L_0^2L_1^2N_2N_4^3 - 2L_0^3L_2N_2N_4^3 - \\
& L_0^3L_1N_3N_4^3 + L_0^4N_4^4
\end{aligned}$$